Evapotranspiration partitioning based on leaf and ecosystem water use efficiency

Liuyang Yu[a,b], Sha Zhou[c], Xiaodong Gao[a,b,d], Xining Zhao[a,b,d], Lei Cheng[e], Kadambot H.M. Siddique[f]

[a] *Institute of Water-saving Agriculture in Arid Areas of China, Northwest A&F University, Yangling 712100, Shaanxi Province, China*

[b] *Key Laboratory of Agricultural Soil and Water Engineering in Arid and Semiarid Areas, Ministry of Education, Northwest A&F University, Yangling 712100, Shaanxi Province, China*

[c] *Department of Earth and Environmental Engineering, Columbia University, New York, New York, 10027, USA*

[d] *Institute of Soil and Water Conservation, Northwest A&F University, Yangling 712100, Shaanxi Province, China*

[e] *Wuhan Univ, State Key Lab Water Resources & Hydropower Engn S, Wuhan 430072, Hubei, Peoples R China*

[f] *The UWA Institute of Agriculture, The University of Western Australia, Perth WA 6001, Australia*

Corresponding author: Institute of Soil and Water Conservation, Northwest A&F University, Xining 26 Road, Yangling 712100, Shaanxi Province, China; *Tel*: 86-13319241600, *Email*: zxn@nwafu.edu.cn (X. Zhao)

Key Points

1. A novel *ET* partitioning method coupling with WUEs at various scales was developed.
2. Magnitudes and trends in *T:ET* were consistent with the results of various *ET* partitioning methods and the known effect from LAI.
3. The novel *ET* partitioning method is not restricted to areas and plant types and improves *T:ET* estimation accuracy in water-limited regions.

Abstract

Partitioning evapotranspiration (*ET)* is essential for improving water resource management and understanding the global hydrological cycle. However, *ET* partitioning in various ecosystems is challenging as some assumptions are restricted to certain areas or plant types. Here, we developed a novel *ET* partitioning method coupling definitions of leaf and ecosystem water use efficiencies (WUE_{leaf} and WUE_{eco}, respectively). We used 25 eddy covariance flux sites for 196 site-years to evaluate *T:ET* characteristics of seven plant functional types (PFTs) at different spatiotemporal scales. The results indicated the spatiotemporal characteristics of WUE_{leaf} and WUE_{eco} were not consistent, resulting in *T:ET* variation in the seven PFTs. Deciduous broadleaf forests showed the highest mean annual *T:ET* (0.67), followed by evergreen broadleaf forests (0.63), grasslands (0.52), evergreen needleleaf forests (0.46), and woody savanna (0.41), and C_3 croplands had higher *T:ET* (0.65) than C_4 croplands (0.48). The annual mean leaf area index (LAI) explained about 26% of the variation in *T:ET*, with the trend in *T:ET* consistent with the known effects of LAI. The overall trends and magnitude of *T:ET* in this study were similar to different results of *ET* partitioning methods globally. Importantly, this method improved *T:ET* estimation accuracy in vegetation-sparse and water-limited areas. Our novel *ET* partitioning method is suitable for estimating *T:ET* at various spatiotemporal scales and provides insight into the conversion of WUE at different scales.

1. Introduction

Evapotranspiration (*ET*)—including evaporation of soil water and water intercepted by the plant canopy (*E*), and stomatal transpiration (*T*)—is crucial for understanding global ecohydrological systems [*Katul et al.,* 2012; *Wang and Dickinson,* 2012; *Kool et al.,* 2014]. Transpiration is directly in connection with biological processes with photosynthesis for plant productivity and usually considered as productive water loss [*Granier et al.,* 1999; *Jasechko et al.,* 2013; *Yi et al.,* 2019]. Enhancing the productive part (*T*) and decreasing the non-productive part (*E*) is critical for the sustainable water resources management in drylands [*Newman et al.,* 2010; *Kool et al.,* 2014]. Therefore, partitioning *ET* into *E* and *T* is essential for land surface process models [*Lawrence et al.,* 2007], quantifying water use efficiency (WUE), and coupling hydrological and biogeochemical cycles [*Austin et al.,* 2004; *Mastrotheodoros et al.,* 2017]. However, partitioning *ET* continuously is challenging in most ecosystems.

Some methods from the site to ecosystem scale have been used to investigate the ratio of *T* to *ET,* denoted as *T:ET*, including sap flow [*Rafi et al*., 2019], stable isotope [*Wang et al.*, 2010; *Xiao et al.*, 2018], eddy covariance [*Paul-Limoges et al.,* 2020], and model simulation [*Gu et al.,* 2018]. Sap flow can continuously record plant transpiration, but it is difficult to scale up to field ecosystems [*Kool et al.,* 2014]. Water stable isotopes for *ET* partitioning are based on differences in the water vapor isotope of *E* and *T*, but this method costs a lot of human and financial resources and makes continuous observation difficult [*Griffis,* 2013; *Xiao et al.,* 2018]. Mechanistic and empirical models can overcome these issues, but the debatable hypothesis [*Schlaepfer et al.,* 2014] and substantial number of parameters [*Kool et al*., 2014] have caused some uncertainties in modeling simulations. Eddy covariance technique is used to measure exchanges of carbon and water flux between atmosphere and underlying surface, and flux networks have been more than 900 sites worldwide [*Baldocchi and Ryu,* 2011; *Zhou et al.,* 2016]. Traditionally, eddy-covariance techniques ignore understory *T* and plant *E* from canopy rainfall interception. A new *ET* partitioning method was introduced by *Scanlon and Sahu* [2008], which assumed that the relationship between *T* and *E* is related to stomatal fluxes and non-stomatal fluxes, and involved the parameter of leaf WUE [*Scanlon and Kustas,* 2010]. However, this

method has not been widely adopted as it requires high frequency (10–20 Hz) data; therefore, some sites in global flux networks cannot be used due to the flux-variance similarity assumption [*Wagle et al.,* 2020]. Zhou *et al.* [2016] introduced a novel *ET* partitioning method based on underlying water use efficiency (uWUE), which is easy to use in practice and can estimate *T:ET* at various spatiotemporal scales [*Berkelhammer et al.,* 2016; *Zhou et al.,* 2016; *Jiang et al.,* 2020], but has some limitations. Firstly, the assumption that $T = ET$ at times during the growing season might be invalid in arid and vegetation-sparse areas, where *E* cannot be ignored. Therefore, this method would overestimate *T:ET* [*Scott and Biederman,* 2017; *Li et al.,* 2019;]. Secondly, a linear relationship between $(1-C_i/C_a)$ and the square root of vapor pressure deficit ($VPD^{0.5}$) is only applicable for C_3 plants, so leaf uWUE is not available for C_4 plants due to the lack of marginal water cost of carbon gain (λ_{cf}) [*Lloyd and Farquhar,* 1994]. Thirdly, the marginal WUE changes when stomata no longer behave optimally under severe water deficit due to limited xylem water transport, the uWUE method is not useful [*Zhou et al.,* 2018].

Here, we developed a novel and simple *ET* partitioning method that accounts for leaf and ecosystem WUE (WUE_{leaf} and WUE_{eco}) and applies to all areas and plant types using accessible half-hourly eddy-covariance flux data. To provide a reliable evidence for the proposed novel *ET* partitioning method, this study aimed to (1) evaluate WUE_{leaf} and WUE_{eco} among plant functional types (PFTs) at spatiotemporal scales, (2) evaluate *T:ET* variation in PFTs at spatiotemporal scales, and (3) evaluate the feasibility of the new *ET* partitioning method and its applicability in arid areas. The proposed method can evaluate characterization of *T:ET* at multiple spatiotemporal scales at global flux tower networks.

2. Methods

The theoretical foundation of water loss from *E*, *T,* and *ET* is associated with non-stomatal, stomatal, and stomatal/non-stomatal mixing behaviors, respectively [*Scanlon and Sahu,* 2008; *Scanlon and Kustas,* 2010]. Transpiration is related to plant and regulated by leaf stomas, while *E* is only related to soil and environmental conditions. According to observation scales and water consumption differences, WUE is defined differently at various spatiotemporal scales. The concept of WUE includes ecosystem WUE (WUE_{eco}), which combines stomatal and non-stomatal mixing behaviors, and ecosystem transpiration efficiency ($iWUE_{eco}$), which is only associated with stomatal behaviors. WUE_{eco} is defined as the ratio of carbon fixation (GPP) to water consumption by the ecosystem (*ET*), and $iWUE_{eco}$ is defined as the ratio of GPP to water consumption via transpiration (*T*). Thus, *T:ET* can be determined from the ratio of WUE_{eco} to $iWUE_{eco}$. WUE_{eco} can be estimated directly from GPP and ET provided by flux-covariance sites. It is difficult to obtain $iWUE_{eco}$ but it can be up-scaled from WUE_{leaf} indirectly. Ecosystem WUE is defined as the ratio of ecosystem GPP of ecosystem to water consumption via evapotranspiration (*ET*), and it can also be decomposed into GPP/T and *T:ET*:

$$WUE_{eco} = \frac{GPP}{ET} = \frac{GPP}{T} \times \frac{T}{ET} = iWUE_{eco} \times \frac{T}{ET} \qquad (1)$$

In this study, evapotranspiration (*ET*) includes transpiration (*T*), soil water evaporation (E_s) and canopy interception evaporation (E_i):

$$ET = T + E_s + E_i \qquad (2)$$

Studies indicated that WUE at the leaf level can be directly up-scaled to the canopy level in a consistent natural environment [*Barton et al.,* 2012; *Linderson et al.,* 2012]. Zhou *et al.* [2016] also tested that uWUE at the leaf level is broadly consistent with the ecosystem level ($GPP \cdot VPD^{0.5}/T$). Thus, ecosystem $iWUE_{eco}$ (GPP/*T*) in Eq. (3), can be approximated the WUE at the leaf level (WUE_{leaf}) [*Cheng et al.,*

2017; *Medlyn et al.,* 2011].

$$iWUE_{eco} = \frac{GPP}{T} = \frac{\int A\,dt}{\int T\,dt} \approx WUE_{leaf} = \frac{A}{T} = \frac{C_a P_a}{1.6\left(VPD + g_1\sqrt{VPD}\right)} \quad (3)$$

where A is leaf net photosynthetic rate (μmol (CO_2) m^{-2} s^{-1}), T is leaf transpiration rate (μmol (H_2O) m^{-2} s^{-1}), P_a is atmospheric pressure (kPa), C_a is ambient atmospheric CO_2 concentration (mol(CO_2) mol^{-1}), VPD is vapor pressure deficit (kPa), and g_1 is an empirical parameter of the stomatal conductance model ($kPa^{0.5}$), representing the exchange rate between carbon uptake and water use [*Knauer et al.,* 2018; *Medlyn et al.,* 2011]. Lin *et al.* [2015] compiled the mean g_1 value of different PFTs using a global-scale extensive field observation dataset. The g_1 values at the fluxnet tower sites in our study were extracted from a global map of g_1 parameters (see Supplementary Information of *Cheng et al.* [2017]) by interpolating g_1 values of different PFTs with a global plant classification map (SYNMAP). The g_1 values at the fluxnet tower sites in our study are shown in Table 1.

Substituting Eq. (3) into Eq. (1):

$$WUE_{eco} = WUE_{leaf} \times \frac{T}{ET} \quad (4)$$

Thus, the *T:ET* can be estimated from the ratio of WUE_{eco} to WUE_{leaf} as follows:

$$\frac{T}{ET} = \frac{WUE_{eco}}{WUE_{leaf}} = \frac{\frac{GPP}{ET}}{\frac{C_a P_a}{1.6\left(VPD + g_1\sqrt{VPD}\right)}} \quad (5)$$

3. Datasets

3.1 Flux tower data

Half-hourly flux-tower dataset from the FLUXNET2015 (https://fluxnet.org) were extracted. Sites were selected with the following data recorded: net solar radiation, air temperature, precipitation, latent heat flux, atmospheric pressure, ambient atmospheric CO_2 concentration, vapor pressure deficit (*VPD*), and estimates of gross primary productivity (GPP). Air temperature and latent heat flux at half-hourly intervals data were used to calculated *ET* (kg H_2O m^{-2} d^{-1}) [*Donatelli et al.,* 2006]. Twenty-five sites (196 site-years) were selected and their specific information were shown in Table 1, and there are 6 PFTs in this study. Cropland were separated by C_3 and C_4 crops. The selected sites are distributed in arid and humid areas, with mean annual precipitation gradients ranging from 380 to 1426 mm (Table 1).

Data quality control and screening were addressed following similar criterion and processes reported in other studies [*Li et al.,* 2019; *Zhou et al.,* 2016]. First, data only at daylight with positive net solar radiation, GPP, *ET*, and *VPD* can be reserved and defective data were excluded. Second, incoming shortwave radiation less than 50 W m^{-2} and sensible heat flux less than 5 W m^{-2} were excluded to avoid stable boundary layer conditions [*Li et at.,* 2019]. The data of rainy days were excluded by referring to *Zhou et al.,* [2015]. Fourth, we only focus on the data of the growing season period and the division of the growing season period was used the method in *Zhou et al.,* [2016]. Finally, daily values were selected to estimate *T:ET* only when the day contains at least 10 half-hourly data.

3.2 Leaf area index (LAI)

In this study, LAI (m^2 m^{-2}) of vegetation was estimated using photosynthetically active radiation data, and the estimation was used the method in *Xu et al.,* [2010].

4. Results and Discussion

4.1 Estimation of WUE_{leaf} and WUE_{eco}

The average and long-term WUE_{eco} and WUE_{leaf} of seven PFTs for the 25 sites are shown in Fig. 1. Overall, the spatiotemporal characteristics of WUE_{eco} and WUE_{leaf} for seven PFTs were not consistent, which is consistent with the findings reported by *Yi et al.* [2019]. For example, deciduous broad forests (4.95 g C kg^{-1} H_2O) and evergreen broad forests (4.97 g C kg^{-1} H_2O) had the highest $WUE_{eco,}$ while evergreen needleleaf forests (11.7 g C kg^{-1} H_2O) and C_4 croplands (11.3 g C kg^{-1} H_2O) had the highest WUE_{leaf}. The inconsistent trend between WUE_{eco} and WUE_{leaf} reflects the proportion of productive and non-productive water consumption in the water cycle across different PFTs. The results also showed that C_4 croplands had higher WUE_{eco} (4.0 g C kg^{-1} H_2O) and WUE_{leaf} (11.3 g C kg^{-1} H_2O) than C_3 croplands (2.8 g C kg^{-1} H_2O and 5.2 g C kg^{-1} H_2O, respectively). The C_4 leaves have higher WUE than C_3 leaves under same conditions due to the CO2 concentration mechanism [*Ghannoum,* 2009]. However, C_4 croplands had much higher WUE_{leaf} than its WUE_{eco} and the WUE_{leaf} of C_3 croplands, indicating that C_4 croplands had lower *T:ET* than C_3 croplands. In addition, the WUE of croplands varies in agricultural systems and is mostly determined by local irrigation and field management practices. For natural vegetation, deciduous broad forests (4.95 g C kg^{-1} H_2O) and evergreen broad forests (4.97 g C kg^{-1} H_2O) had higher WUE_{eco} than evergreen needleleaf forests (4.2 g C kg^{-1} H_2O) and grasslands (2.4 g C kg^{-1} H_2O), which were consistent with the studied model simulation [*Gu et al.,* 2018] and global satellite data [Huang *et al.,* 2017]. Broad forests had higher carbon uptake capacity than evergreen needleleaf forests due to their larger leaf area (Fig. 2). Compared to grasslands, forests had higher WUE_{eco}, which is likely due to their (1) lower *E,* as their large canopy and tree height reduces the gradient in *VPD* between the atmosphere and soil surface [*Brutsaert,* 2005] and/or (2) lower *T* due to the distribution of leaf stomata. In most herbs, stomata exist on both the adaxial and abaxial leaf surfaces, while in many trees, stomata only exist on the adaxial leaf surface [*Taiz and Zeiger,* 2006]. In this study, woody savannas had the lowest WUE_{eco} (1.8 g C kg^{-1} H_2O) and WUE_{leaf} (4.8 g C kg^{-1} H_2O). The US_SRM and US_Ton sites for woody savannas belonged to arid and semiarid areas; their low WUE_{eco} and WUE_{leaf} values have been attributed to low carbon uptake and large soil evaporation [*Scott and Biederman,* 2017; *Wang et al.,* 2016].

Multi-year and interannual variations in WUE_{eco} and WUE_{leaf} for the DE_Gri (GRA), IT_Cpz (EBF), FR_Fon (DBF), US_Ne1 (CRO), US_NR1 (ENF), US_SRM (WSA) sites were estimated daily (Fig. 2). The multi-year variation was small for each site, but inter-sites were large for WUE_{eco}, $WUE_{leaf,}$ and GPP. Similar results were reported in *Nelson et al.* [2020], indicating that *T:ET* differs more from one site to another than between years for the same site. For all PFTs, the daily variation trend in WUE_{eco} is consistent with that of GPP, but WUE_{leaf} showed high-frequency fluctuations over time. The high-frequency variation of WUE_{leaf} is the main reason for the high variation in the estimated daily *T:ET.* In this study, the stomatal conductance model was used to estimated WUE_{leaf} half-hourly, and g_1 is constant when vegetation type and site are determined. Although the variations in ambient atmospheric CO_2 concentration and atmospheric pressure were small on a daily scale, studies have shown that ambient atmospheric CO_2 concentration has a significant effect on WUE_{leaf} [*Knauer et al.,* 2017; *Onoda et al.,* 2009]. The high-frequency variation is mostly attributed to variation in *VPD*, which is easily affected

by daily climate factors, such as light, humidity, and temperature. Similarly, *Yi et al.* [2019] indicated that WUE_{leaf} was most sensitive to variations in *VPD*, accounting for 86% of influence factors of *VPD*, soil moisture, and ambient atmospheric CO_2 concentration.

4.2 Estimation of *T:ET*

The annual mean *T:ET* varied greatly among 196 site-years with seven PFTs (Fig. 3). Overall, the mean *T:ET* among the 196 site-years was 0.54 (range 0.4–0.67), which is very close to results (0.57, range 0.5–0.64) on a global terrestrial scale [*Wei et al., 2017*]. In this study, deciduous broad forests had the highest average *T:ET* (0.67, range 0.50–0.78), with the trend and magnitude similar to the results of a global meta-analysis (0.67) [*Schlesinger and Jasechko,* 2014], transpiration estimation algorithm (TEA) method (0.7) [*Nelson et al., 2018*] and modeling study (0.6) [*Gu et al.,* 2018]. However, Zhou *et al.* [2016] reported that deciduous broad forests (0.52±0.08) had the lowest *T:ET* among all PFTs, being lower than those reported by *Schlesinger and Jasechko* [2014] in a global synthesis of 81 studies on *ET* partitioning. The reason for underestimating *T:ET* of deciduous broad forests was explained in *Zhou et al.* [2016]. The estimated annual *T:ET* for ENF (mean 0.46) is lower than that reported (0.55) by *Schlesinger and Jasechko* [2014] but the values for each site in this study (0.34–0.61) were all within the range for ENF (0.3–0.7). The reason for underestimation may be due to parameter g_1 variation among the four evergreen needleleaf forest sites. Our study had two sites (CA_NS3 and US_NR1) with small g_1 values (2.9 and 2.6, respectively). A low g_1 would be accompanied by high WUE_{leaf}, resulting in low *T:ET*. The annual *T:ET* of grasslands varied little (0.52, range 0.38–0.67), compared with 0.56±0.05 [*Zhou et al.,* 2016] and 0.57±0.19 [*Schlesinger and Jasechko*, 2014], because we included two grasslands located in arid areas and their perennial average *T:ET* were 0.45 and 0.56 for US_Wkg and US_SRG sites, respectively. Thus, the estimated *T:ET* by using our method is very close to that reported in the published researches for deciduous broad forests, evergreen needleleaf forest, and grasslands. Moreover, this study showed that C_3 croplands had higher *T:ET* (0.65) than C_4 croplands (0.48), which is consistent with those for wheat (C_3) and maize (C_4) using *ET* partitioning methods with a two-source model or isotope approach [*Wei et al.,* 2018]. However, the *ET* partitioning method used by *Zhou et al.* [2016] showed that C_4 croplands had higher *T:ET* (0.69) than C_3 croplands (0.62). The reason why *T:ET* differs in agriculture systems may be due to human factors, such as irrigation, mulching or fertilizer. In addition, two woody savannas (US_Ton and US_SRM) located in semiarid and arid sites had an average *T:ET* of 0.41 (range 0.39–0.43), which is consistent with that (0.48±0.12) reported by *Schlesinger and Jasechko* [2014].

Seasonal and interannual variations in *T:ET* for DE_Gri (GRA), IT_Cpz (EBF), FR_Fon (DBF), US_Ne1 (CRO), US_NR1 (ENF), and US_SRM (WSA) were estimated daily (Fig. 4). Overall trends in seasonal *T:ET* characteristics for six PFTs were similar to those in the TEA and uWUE methods [*Nelson et al.*, 2020]. We selected three sites and years (DE_Gri, US_Ne1, and US_NR1) that were also used in a novel *ET* partitioning method based on soil and canopy conductances [*Li et al.,* 2019] and compared their *T:ET* trends and characteristics within and between years. The three sites showed consistent trends in *T:ET* characteristics, albeit slightly higher in *Li et al.* [2019] because they did not include evaporation from canopy interception.

The seasonal patterns of *T:ET* differed for the six PFTs. For grasslands at the DE_Gri site, *T:ET* increased to 0.8 over time but rapidly declined with the harvest of herbage, which occurred several times a year. For croplands, maize grew faster than the other natural vegetation, and *T* rapidly reached its maximum. The daily variation in *T:ET* at the US_Ne1 site followed a single-peak pattern within a growing season. For evergreen broad forests at the IT_Cpz site, the *T:ET* was mostly above 0.4, with an unobvious peak and large variation in daily *T:ET* during the growing season. For evergreen needleleaf forests at the US_NR1 site, *T:ET* was below 0.2 in the early

growing season, and showed high-frequency fluctuations, reaching a peak value of about 0.54 during the growing season. The reasons for the high-frequency fluctuations in *T:ET* across plant types are provided in section 4.1. Moreover, large daily variations in *T:ET* can be influenced other biotic/abiotic factors, for example, soil water content, vegetation coverage, and plant phenology [*Berkelhammer et al.,* 2016; *Gao et al.,* 2019; *Oishi et al.,* 2008].

4.3 Evaluation of the *ET* partitioning method

The relationship between mean growing season LAI and annual *T:ET* shows a significant R^2 of linear regression ($p < 0.01$) (Fig. 5). This result is similar to that of *Li et al.* [2019] and *Gu et al.* [2018], but with improved correlation coefficients. However, the low R^2 of 0.26 suggests the mean growing season LAI explains small (26%) variations in mean annual *T:ET* across biomes, indicating that other biological and non-biological factors affect ET variation in addition to LAI in global ecosystem. Ambient atmospheric conditions (e.g., *VPD* and precipitation), soil moisture, and plant phenology are important factors affecting high *T:ET* variation at daily or seasonal scales [*Good et al.,* 2014; *Scott and Biederman,* 2017; *Zhao et al.,* 2018]. Another reason is that the mean LAI values of the growing season but not the whole growing season, including the early growing season, were selected in this study. Scott and Biederman [2017] indicated that a larger percentage of *T:ET* variation is explained by a commonly used power function with LAI rather than a linear relationship early in the growing season. Overall, the correlation between LAI and *T:ET* further demonstrates the reliability of this new *ET* partitioning method.

The mean annual *T:ET* across 196 site-years was compared with previously published estimates using four methods (isotope, modeling, flux data, and meta-analysis). Inter-comparison of various *ET* partitioning methods showed a spread in magnitudes of *T:ET* from 0.38 to 0.75 (Fig. 6). The overall *T:ET* across the 196 site-years in this study was 0.54 (range 0.40–0.67). On the whole, the average *T:ET* values were slightly lower than studies, although the ranges of *T:ET* for several PFTs were all within the global given reasonable interval. There may be several possible reasons for this. Firstly, many published studies ignore the rainfall evaporation intercepted by the plant canopy, which would overestimate *T:ET* [*Baldocchi,* 2014; *Li et al*., 2019]. Moreover, measurement of *E* and *T* separately will overestimate the proportion of *T* in *ET* [*Gu et al.*, 2018]. Finally, different research regions (such as those that focus only on non-limited water regions) and various scales may influence the results of *T:ET*; for example, the isotope-based approach overestimates *T:ET*, which is constrained by hydrologic decoupling [*Jasechko et al.*, 2013]. Wang *et al.* [2014] indicated that large variabilities and observation uncertain across sites could generate a large *T:ET* range. Similarly, Nelson *et al.* [2020] reported a 0.45–0.77 spread in magnitude of *T:ET* using three *ET* partitioning methods based on fluxnet data, despite plausible and qualitatively consistent *T* and *T:ET* patterns. Therefore, various ET portioning methods and measurement techniques should be used to reduce uncertainties in *T* estimation [*Rafi et al.,* 2019].

We used three *ET* partitioning methods to compare monthly and growing season *T:ET* in two arid grasslands (Table 2). One of the methods —proposed by *Scott and Bieberman* [2017]—is a reliable method for estimating *T:ET* at water-limited sites. In general, the three *ET* partitioning methods produced consistent *T:ET* at the seasonal scale. The monthly and whole growing season *T:ET* values from our method were similar to those of *Scott and Bieberman* [2017], with small differences of +1.8% and –0.3% for the US_SRG and US_Wkg sites, respectively. Unsurprisingly, Zhou et al.'s [2015] method overestimated growingseason *T:ET* at the at US_Wkg site by 37.8%, relative to that in *Scott and Bieberman* [2017]. Moreover, we compared the daily *T:ET* estimation of our method and Zhou et al.'s method at two arid grassland sites (Figs 7 and 8). The Pearson's correlation coefficients of *T:ET* on a daily scale for the two methods were 0.95 and 0.85 at the US_SRG and US_Wkg sites, respectively. The overall *T:ET* trends on a daily scale were consistent for the two methods,

but Zhou et al.'s method produced higher *T:ET* estimation values than our method because their assumption that *T* equals *ET* throughout the growing season is not valid for arid and vegetation-sparse areas. Our *ET* partitioning method is not restricted to arid and vegetation-sparse areas and improved the *T:ET* estimation accuracy in water-limited regions.

4.4 Implications and limitations

This study developed a novel method of *ET* partitioning based on the relationship between WUE_{leaf} and WUE_{eco} by using easily available eddy-covariance data. This method has several advantages over other *ET* partitioning techniques that use eddy-covariance measurements. Unlike *Zhou et al.* [2016] and *Scott and Biederman* [2017], our novel method is applicable to all regions and PFTs and not limited by local soil moisture in dry or wet areas. Unlike *Li et al.* [2019], our method incorporates evaporation from canopy interception. Importantly, our method can easily estimate *T:ET* at spatiotemporal scales using meaningful ecological interpretations of WUE_{eco} and WUE_{leaf} through reliable theoretical derivation. Moreover, this method helps understand the upscaling or downscaling of WUEs at different scales.

However, there are several limitations to this study. First, uncertainty in GPP and ET estimations would result in some uncertainty in WUE_{eco} and hence *T:ET*. Second, the lack of direct observations of *E* and *T* at the flux tower sites to validate our partitioning method. Although the comparison with other ET partitioning methods lend considerable support for our method, we also find a few inconsistent results and there is no consistent conclusion as to which *ET* partitioning method or measurement technique is the most accurate [*Kool et al.,* 2014]. Thirdly, we assumed that WUE_{leaf} can be used to approximate $iWUE_{eco}$, which may not be true at sites with mixed vegetation types with distinct WUE_{leaf} or heterogeneous environmental conditions, such as *VPD* and light density, leading to large variations in WUE_{leaf} within the site. Finally, the g_1 values were determined from different PFTs and land cover maps. As g_1 is predicted to change with moisture index and temperature [*Lin et al.,* 2015], using a constant g_1 value at each site may lead to some uncertainty in WUE_{leaf} and hence *T:ET*. The reason for not considering soil moisture and temperature is to retain a simple and available parameter in the *T:ET* model.

5. Conclusion

Half-hourly flux data from 196 eddy covariance site-years was used to develop a novel *ET* partitioning method coupled with WUE at various scales. According to WUE based on water consumption, *T:ET* equals the ratio of WUE_{eco} to WUE_{leaf} numerically through reasonable derivation, and WUE_{eco} and WUE_{leaf} can be easily calculated from available data provided by flux sites. The spatiotemporal characteristics of WUE_{eco} and WUE_{leaf} for seven PFTs were not consistent, which reflects the proportion of productive and non-productive water consumption across PFTs. For natural vegetation, deciduous broad forests and evergreen broad forests had higher WUE_{eco} than evergreen needleleaf forests and grasslands, but evergreen needleleaf forests had the highest WUE_{leaf}. For agricultural systems, C_4 croplands had higher WUE_{eco} and WUE_{leaf} than C_3 croplands due to the CO_2-concentrating mechanism. Moreover, *T:ET* characteristics varied among PFTs. Deciduous broadleaf forests had the highest mean annual *T:ET* (0.67), followed by evergreen broadleaf forests (0.63), grasslands (0.52), evergreen needleleaf forests (0.46), and woody savannas (0.41). The C_3 croplands (0.65) had higher *T:ET* ratios than C_4 croplands (0.48). We also examined the feasibility and reliability of our *ET* partitioning method—the trends and magnitudes in *T:ET* were consistent with those of other *ET* partitioning methods and the known effect from LAI. Furthermore, our method improved *T:ET* estimation accuracy in vegetation-sparse and water-limited areas. Thus, this method is sound in principle, in addition, it is easy to used and widely implemented for all regions and plant types using data from global flux tower networks. Moreover, this method provides new

insights into the conversion of WUE at different scales.

Acknowledgments

Data for these flux sites are archived at https://fluxnet.org/sites/site-summary and freely obtainable. We acknowledge funding from the National Key Research and Development Program (2016YFC0400204), the National Natural Science Foundation of China (41571506, 41771316, 51579212), the Shaanxi Innovative Research Team for Key Science and Technology (2017KCT-15), the '111'Project (B12007), and CAS "Youth Scholar of West China" Program (XAB2018A04).

References

Austin, A. T., L. Yahdjian, J. M. Stark, J. Belnap, A. Porporato, U. Norton, D. A. Ravetta, and S. M. Schaeffer (2004), Water pulses and biogeochemical cycles in arid and semiarid ecosystems, *Oecologia*, *141*(2), 221-235.

Baldocchi, D. (2014), Measuring fluxes of trace gases and energy between ecosystems and the atmosphere - the state and future of the eddy covariance method, *Glob. Change Biol.*, *20*(12), 3600-3609.

Baldocchi, D., and Y. Ryu (2011), A Synthesis of Forest Evaporation Fluxes - from Days to Years - as Measured with Eddy Covariance, in *Forest Hydrology and Biogeochemistry: Synthesis of Past Research and Future Directions*, edited by D. F. Levia, D. CarlyleMoses and T. Tanaka, pp. 101-116, Springer, Po Box 17, 3300 Aa Dordrecht, Netherlands.

Barton, C. V. M., et al. (2012), Effects of elevated atmospheric CO_2 on instantaneous transpiration efficiency at leaf and canopy scales in Eucalyptus saligna, *Glob. Change Biol.*, *18*(2), 585-595.

Berkelhammer, M., D. C. Noone, T. E. Wong, S. P. Burns, J. F. Knowles, A. Kaushik, P. D. Blanken, and M. W. Williams (2016), Convergent approaches to determine an ecosystem's transpiration fraction, *Global Biogeochemical Cycles*, *30*(6), 933-951.

Brutsaert, W., 2005. Hydrology – An Introduction. Cambridge University Press, New-York

Cheng, L., L. Zhang, Y. P. Wang, J. G. Canadell, F. H. S. Chiew, J. Beringer, L. H. Li, D. G. Miralles, S. L. Piao, and Y. Q. Zhang (2017), Recent increases in terrestrial carbon uptake at little cost to the water cycle, *Nat. Commun.*, *8*, 10.

Donatelli, M., G. Bellocchi, and L. Carlini (2006), Sharing knowledge via software components: Models on reference evapotranspiration, *Eur. J. Agron.*, *24*(2), 186-192.

Gao, L., P. Zhao, S. Kang, S. Li, L. Tong, R. Ding, and H. Lu (2019), Surface soil water content dominates the difference between ecosystem and canopy water use efficiency in a sparse vineyard, *Agric. Water Manage.*, *226*, 105817.

Ghannoum, O. (2009), C4 photosynthesis and water stress, *Ann. Bot.*, *103*(4), 635-644.

Good, S. P., K. Soderberg, K. Y. Guan, E. G. King, T. M. Scanlon, and K. K. Caylor (2014), 2H isotopic flux partitioning of evapotranspiration over a grass field following a water pulse and subsequent dry down, *Water Resour. Res.*, *50*(2), 1410-1432.

Granier, A., N. Breda, P. Biron, and S. Villette (1999), A lumped water balance model to evaluate duration and intensity of drought constraints in forest stands, *Ecol. Model.*, *116*(2-3), 269-283.

Griffis, T. J. (2013), Tracing the flow of carbon dioxide and water vapor between the biosphere and atmosphere: A review of optical isotope techniques and their application, *Agric. For. Meteorol.*, *174*, 85-109.

Gu, C. J., J. Z. Ma, G. F. Zhu, H. Yang, K. Zhang, Y. Q. Wang, and C. L. Gu (2018), Partitioning evapotranspiration using an optimized satellite-based ET model across biomes, *Agric. For. Meteorol.*, *259*, 355-363.

279 Huang, L., B. He, L. Han, J. J. Liu, H. Y. Wang, and Z. Y. Chen (2017), A global examination of the response of ecosystem water-use
280 efficiency to drought based on MODIS data, *Sci. Total Environ.*, *601*, 1097-1107.
281 Jasechko, S., Z. D. Sharp, J. J. Gibson, S. J. Birks, Y. Yi, and P. J. Fawcett (2013), Terrestrial water fluxes dominated by transpiration,
282 *Nature*, *496*(7445), 347-+.
283 Jiang, S., C. Liang, N. Cui, L. Zhao, C. Liu, Y. Feng, X. Hu, D. Gong, and Q. Zou (2020), Water use efficiency and its drivers in four
284 typical agroecosystems based on flux tower measurements, Agric. For. Meteorol., 295.
285 Katul, G. G., R. Oren, S. Manzoni, C. Higgins, and M. B. Parlange (2012), Evapotranspiration: a process driving mass transport and
286 energy exchange in the soil-plant-atmosphere-climate system., *Rev. Geophys.*, *50*, 25.
287 Knauer, J., et al. (2018), Towards physiologically meaningful water-use efficiency estimates from eddy covariance data, *Glob. Change*
288 *Biol.*, *24*(2), 694-710.
289 Knauer, J., S. Zaehle, M. Reichstein, B. E. Medlyn, M. Forkel, S. Hagemann, and C. Werner (2017), The response of ecosystem water-use
290 efficiency to rising atmospheric CO_2 concentrations: sensitivity and large-scale biogeochemical implications, *New Phytol.*, *213*(4),
291 1654-1666.
292 Kool, D., N. Agam, N. Lazarovitch, J. L. Heitman, T. J. Sauer, and A. Ben-Gal (2014), A review of approaches for evapotranspiration
293 partitioning, *Agric. For. Meteorol.*, *184*, 56-70.
294 Lawrence, D. M., P. E. Thornton, K. W. Oleson, and G. B. Bonan (2007), The partitioning of evapotranspiration into transpiration, soil
295 evaporation, and canopy evaporation in a GCM: Impacts on land-atmosphere interaction, *J. Hydrometeorol.*, *8*(4), 862-880.
296 Li, X., P. Gentine, C. J. Lin, S. Zhou, Z. Sun, Y. Zheng, J. Liu, and C. M. Zheng (2019), A simple and objective method to partition
297 evapotranspiration into transpiration and evaporation at eddy-covariance sites, *Agric. For. Meteorol.*, *265*, 171-182.
298 Lin, C. J., P. Gentine, Y. F. Huang, K. Y. Guan, H. Kimm, and S. Zhou (2018), Diel ecosystem conductance response to vapor pressure
299 deficit is suboptimal and independent of soil moisture, *Agric. For. Meteorol.*, *250*, 24-34.
300 Lin, Y. S., et al. (2015), Optimal stomatal behaviour around the world, *Nat. Clim. Chang.*, *5*(5), 459-464.
301 Linderson, M. L., T. N. Mikkelsen, A. Ibrom, A. Lindroth, H. Ro-Poulsen, and K. Pilegaard (2012), Up-scaling of water use efficiency
302 from leaf to canopy as based on leaf gas exchange relationships and the modeled in-canopy light distribution, *Agric. For. Meteorol.*,
303 *152*, 201-211.
304 Lloyd, J., and G. D. Farquhar (1994), C13 distrimination during CO_2 assimilation by the terrestrail biosphere, *Oecologia*, *99*(3-4), 201-
305 215.
306 Mastrotheodoros, T., C. Pappas, P. Molnar, P. Burlando, T. F. Keenan, P. Gentine, C. M. Gough, and S. Fatichi (2017), Linking plant
307 functional trait plasticity and the large increase in forest water use efficiency, *J. Geophys. Res.-Biogeosci.*, *122*(9), 2393-2408.
308 Maxwell, R. M., and L. E. Condon (2016), Connections between groundwater flow and transpiration partitioning, *Science*, *353*(6297),
309 377-380.
310 Medlyn, B. E., R. A. Duursma, D. Eamus, D. S. Ellsworth, I. C. Prentice, C. V. M. Barton, K. Y. Crous, P. de Angelis, M. Freeman, and L.
311 Wingate (2011), Reconciling the optimal and empirical approaches to modelling stomatal conductance, *Glob. Change Biol.*, *17*(6),
312 2134-2144.
313 Nelson, J. A., N. Carvalhais, M. Cuntz, N. Delpierre, J. Knauer, J. Ogee, M. Migliavacca, M. Reichstein, and M. Jung (2018), Coupling
314 Water and Carbon Fluxes to Constrain Estimates of Transpiration: The TEA Algorithm, J. Geophys. Res.-Biogeosci., 123(12), 3617-

3632.

Nelson, J. A., et al. (2020), Ecosystem transpiration and evaporation: Insights from three water flux partitioning methods across FLUXNET sites, Glob. Change Biol.

Newman, B. D., D. D. Breshears, and M. O. Gard (2010), Evapotranspiration Partitioning in a Semiarid Woodland: Ecohydrologic Heterogeneity and Connectivity of Vegetation Patches, *Vadose Zone J.*, *9*(3), 561-572.

Oishi, A. C., R. Oren, and P. C. Stoy (2008), Estimating components of forest evapotranspiration: A footprint approach for scaling sap flux measurements, *Agric. For. Meteorol.*, *148*(11), 1719-1732.

Onoda, Y., T. Hirose, and K. Hikosaka (2009), Does leaf photosynthesis adapt to CO_2-enriched environments? An experiment on plants originating from three natural CO_2 springs, *New Phytol.*, *182*(3), 698-709.

Paul-Limoges, E., S. Wolf, F. D. Schneider, M. Longo, P. Moorcroft, M. Gharun, and A. Damm (2020), Partitioning evapotranspiration with concurrent eddy covariance measurements in a mixed forest, *Agric. For. Meteorol.*, *280*, 12.

Rafi, Z., et al. (2019), Partitioning evapotranspiration of a drip-irrigated wheat crop: Inter-comparing eddy covariance-, sap flow-, lysimeter- and FAO-based methods, *Agric. For. Meteorol.*, *265*, 310-326.

Scanlon, T. M., and P. Sahu (2008), On the correlation structure of water vapor and carbon dioxide in the atmospheric surface layer: A basis for flux partitioning, *Water Resour. Res.*, *44*(10), 15.

Scanlon, T. M., and W. P. Kustas (2010), Partitioning carbon dioxide and water vapor fluxes using correlation analysis, *Agric. For. Meteorol.*, *150*(1), 89-99.

Schlaepfer, D. R., B. E. Ewers, B. N. Shuman, D. G. Williams, J. M. Frank, W. J. Massman, and W. K. Lauenroth (2014), Terrestrial water fluxes dominated by transpiration: Comment, *Ecosphere*, *5*(5), 9.

Schlesinger, W. H., and S. Jasechko (2014), Transpiration in the global water cycle, *Agric. For. Meteorol.*, *189*, 115-117.

Scott, R. L., and J. A. Biederman (2017), Partitioning evapotranspiration using long-term carbon dioxide and water vapor fluxes, *Geophys. Res. Lett.*, *44*(13), 6833-6840.

Taiz, L., and E. Zeiger (2006), Plant Physiology, *Quarterly Review of Biology*, *167*(4), 161-168.

Wagle, P., T. H. Skaggs, P. H. Gowda, B. K. Northup, and J. P. S. Neel (2020), Flux variance similarity-based partitioning of evapotranspiration over a rainfed alfalfa field using high frequency eddy covariance data, *Agric. For. Meteorol.*, *285*, 9.

Wang, K. C., and R. E. Dickinson (2012), A review of global terrestrial evapotranspiration: observation, modeling, climatology, and climatic variability, *Rev. Geophys.*, *50*, 54.

Wang, L., H. Z. Liu, and C. Bernhofer (2016), Grazing intensity effects on the partitioning of evapotranspiration in the semiarid typical steppe ecosystems in Inner Mongolia, *Int. J. Climatol.*, *36*(12), 4130-4140.

Wang, L., K. K. Caylor, J. C. Villegas, G. A. Barron-Gafford, D. D. Breshears, and T. E. Huxman (2010), Partitioning evapotranspiration across gradients of woody plant cover: Assessment of a stable isotope technique, *Geophys. Res. Lett.*, *37*, 7.

Wang, L. X., S. P. Good, and K. K. Caylor (2014), Global synthesis of vegetation control on evapotranspiration partitioning, *Geophys. Res. Lett.*, *41*(19), 6753-6757.

Wei, Z. W., K. Yoshimura, L. X. Wang, D. G. Miralles, S. Jasechko, and X. H. Lee (2017), Revisiting the contribution of transpiration to global terrestrial evapotranspiration, Geophys. Res. Lett., 44(6), 2792-2801.

Wei, Z. W., X. H. Lee, X. F. Wen, and W. Xiao (2018), Evapotranspiration partitioning for three agro-ecosystems with contrasting

moisture conditions: a comparison of an isotope method and a two-source model calculation, *Agric. For. Meteorol.*, *252*, 296-310.

Xiao, W., Z. W. Wei, and X. F. Wen (2018), Evapotranspiration partitioning at the ecosystem scale using the stable isotope method-A review, *Agric. For. Meteorol.*, *263*, 346-361.

Xu, D. Y., X. W. Kang, D. F. Zhuang, and J. J. Pan (2010), Multi-scale quantitative assessment of the relative roles of climate change and human activities in desertification - A case study of the Ordos Plateau, China, *J. Arid. Environ.*, *74*(4), 498-507.

Yi, K., J. T. Maxwell, M. K. Wenzel, D. T. Roman, P. E. Sauer, R. P. Phillips, and K. A. Novick (2019), Linking variation in intrinsic water-use efficiency to isohydricity: a comparison at multiple spatiotemporal scales, *New Phytol.*, *221*(1), 195-208.

Zhao, P., S. Z. Kang, S. Li, R. S. Ding, L. Tong, and T. S. Du (2018), Seasonal variations in vineyard ET partitioning and dual crop coefficients correlate with canopy development and surface soil moisture, *Agric. Water Manage.*, *197*, 19-33.

Zhou, S., B. Yu, Y. F. Huang, and G. Q. Wang (2015), Daily underlying water use efficiency for AmeriFlux sites, *J. Geophys. Res.-Biogeosci.*, *120*(5), 887-902.

Zhou, S., B. F. Yu, Y. Zhang, Y. F. Huang, and G. Q. Wang (2016), Partitioning evapotranspiration based on the concept of underlying water use efficiency, *Water Resour. Res.*, *52*(2), 1160-1175.

Zhou, S., B. Yu, Y. Zhang, Y. Huang, and G. Wang (2018), Water use efficiency and evapotranspiration partitioning for three typical ecosystems in the Heihe River Basin, northwestern China, Agric. For. Meteorol., 253-254, 261-273.

366 **Figure 1.** Distribution of mean ecosystem (WUE_{eco}) and leaf water use efficiency (WUE_{leaf}) for 25 sites across seven plant functional types

367 (PFTs). The *n* value above each bar represents the sample sizes of sites. The bars represent standard deviations of WUE_{eco} and WUE_{leaf} for

368 each PFT.

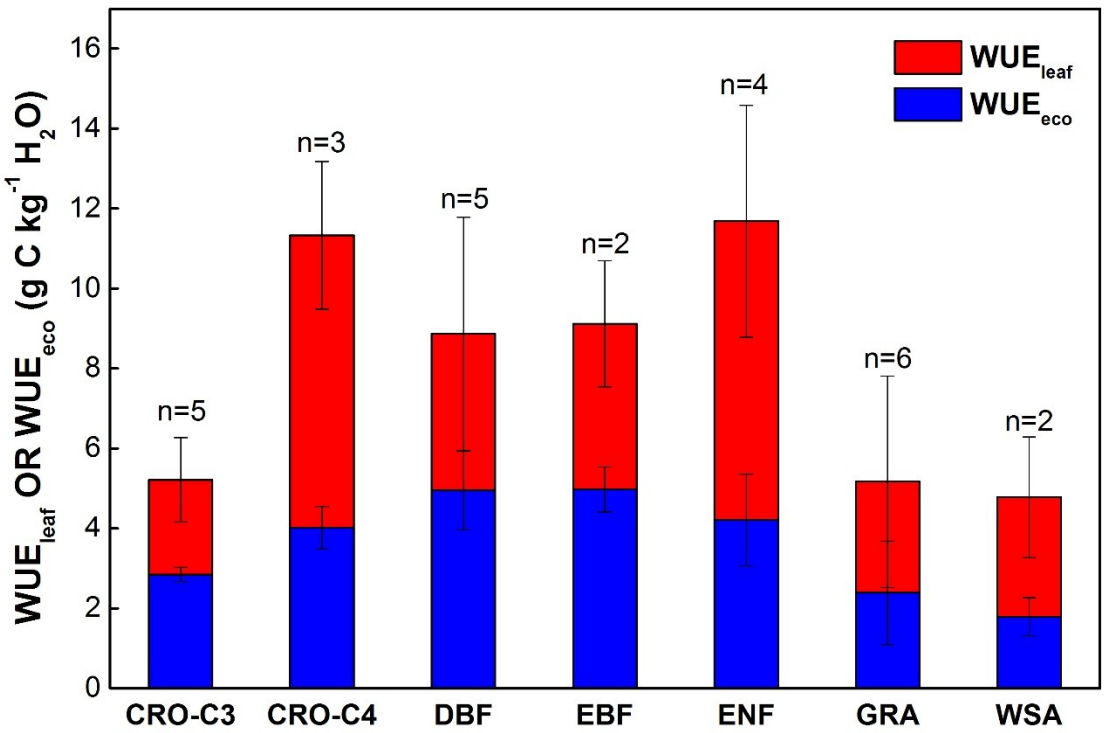

369

370

371 **Figure 2.** Seasonal and interannual variation of gross primary productivity (GPP), ecosystem (WUE_{eco}), and leaf water use efficiency

372 (WUE_{leaf}) at the daily scale for the DE_Gri (GRA), IT_Cpz (EBF), FR_Fon (DBF), US_Ne1 (CRO), US_NR1 (ENF), and US_SRM

373 (WSA) sites.

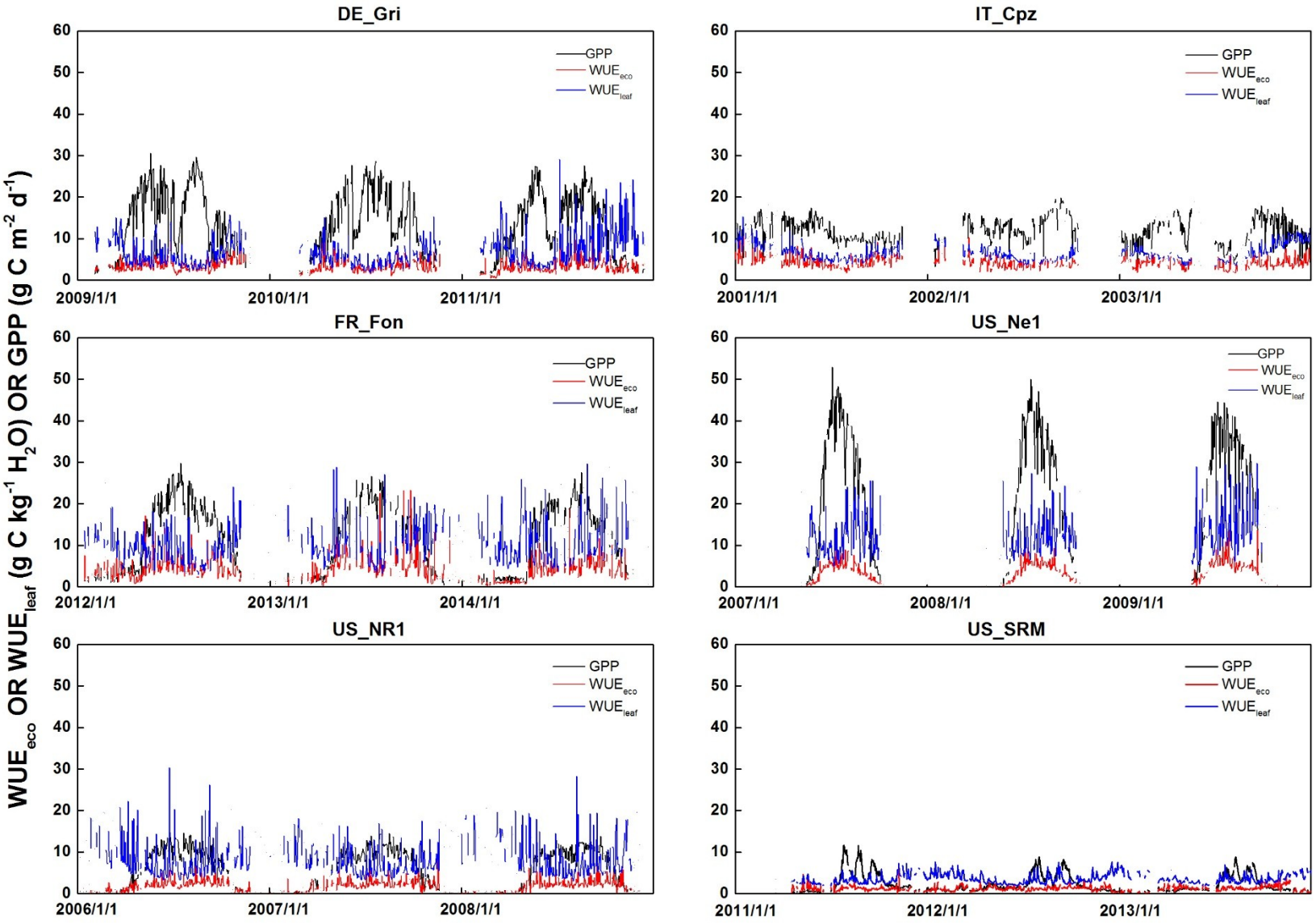

374

375

376 **Figure 3.** Characteristics of *T:ET* of various plant functional types (PFTs) for the 196 site-years. The square and solid lines in the boxes

377 represent the average and median values, the upper and lower error bars represent the quantiles of 75 th and 25th. The *n* values below boxes

378 represents the sample sizes of sites.

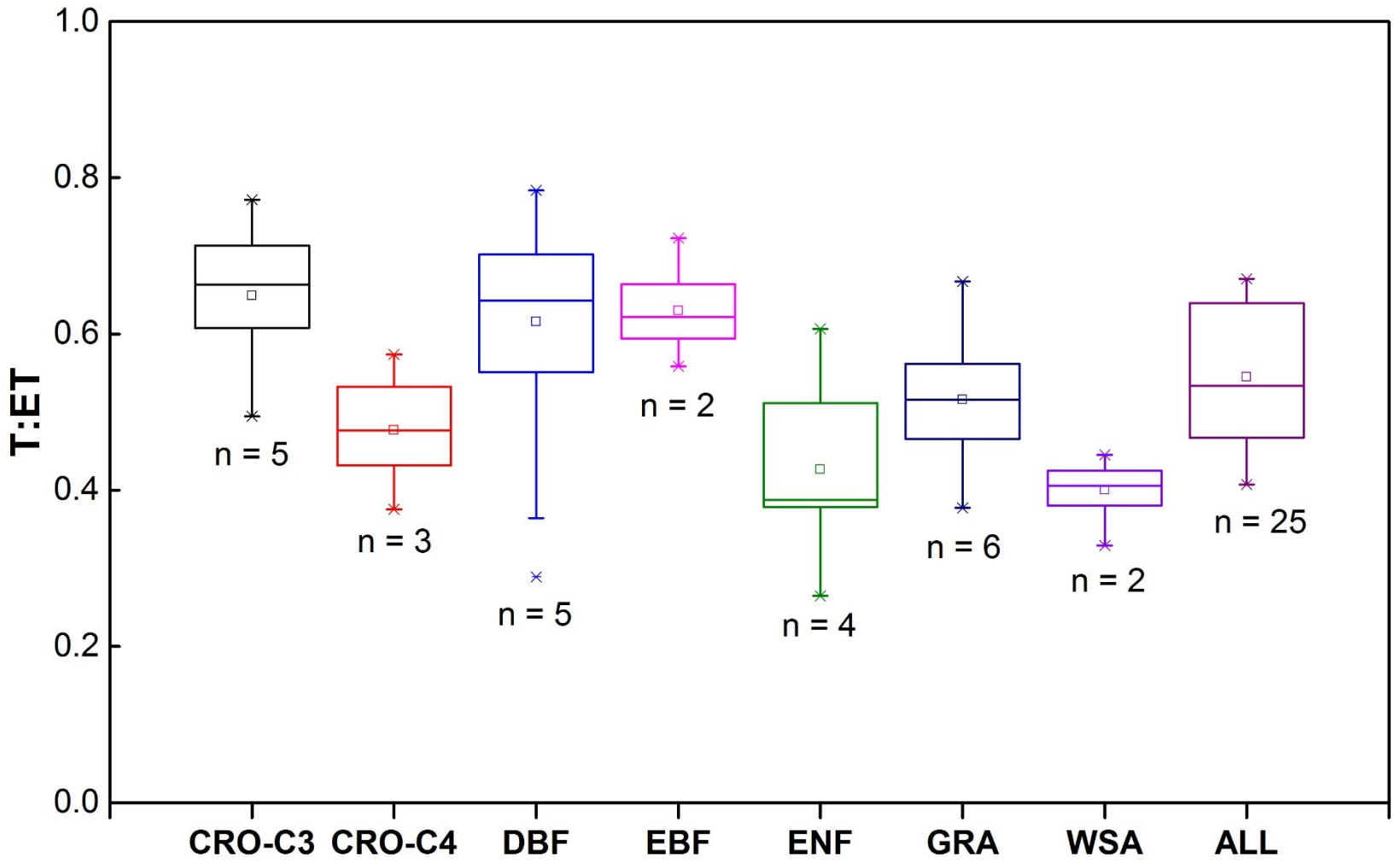

379

380

381 **Figure 4.** Interannual and seasonal and *T:ET* characteristics daily for the DE_Gri (GRA), IT_Cpz (EBF), FR_Fon (DBF), US_Ne1 (CRO),

382 US_NR1 (ENF), and US_SRM (WSA) sites.

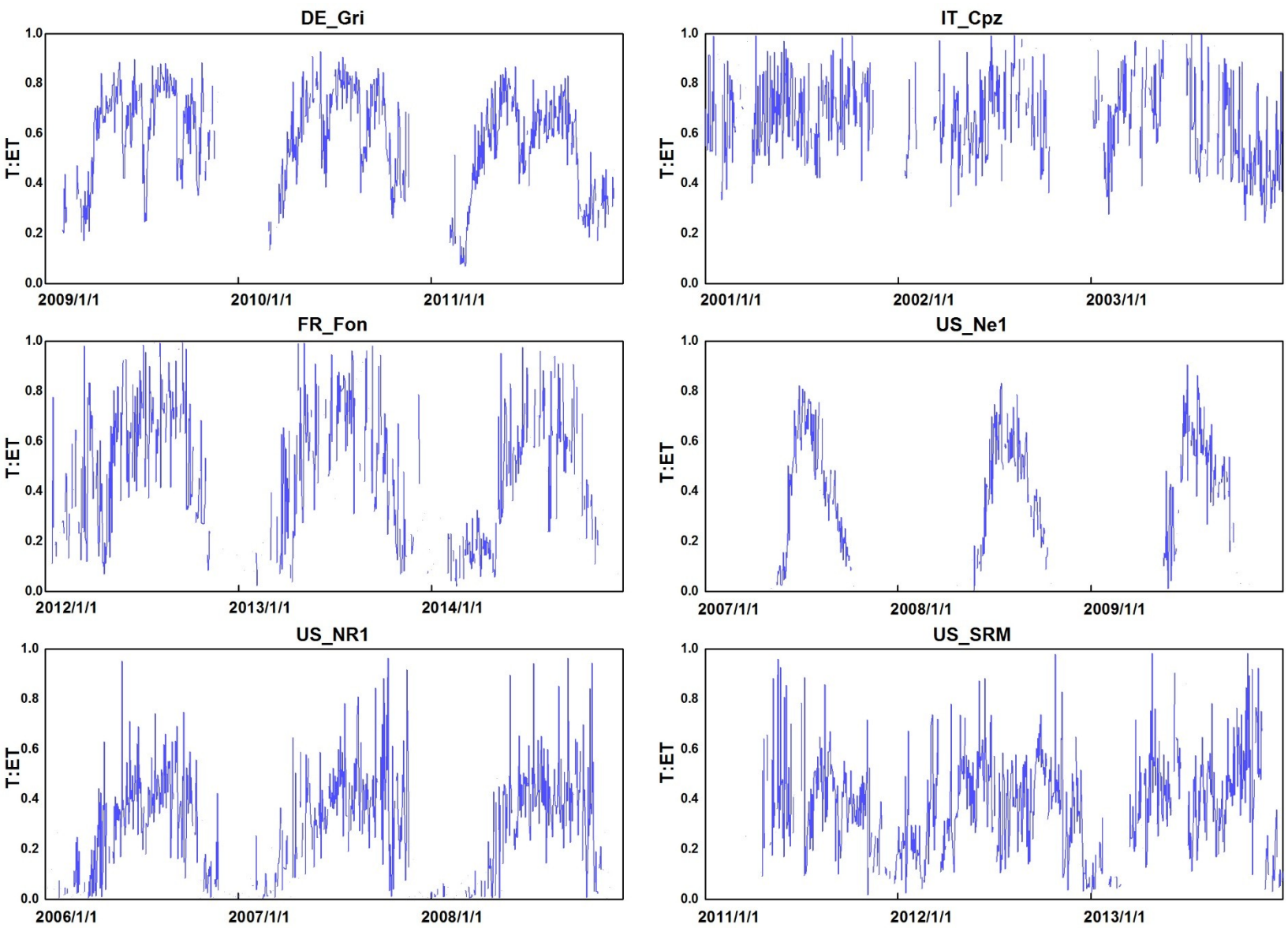

383

384

385 **Figure 5.** The relationship between mean growing season leaf area index (LAI) and mean annual *T:ET*.

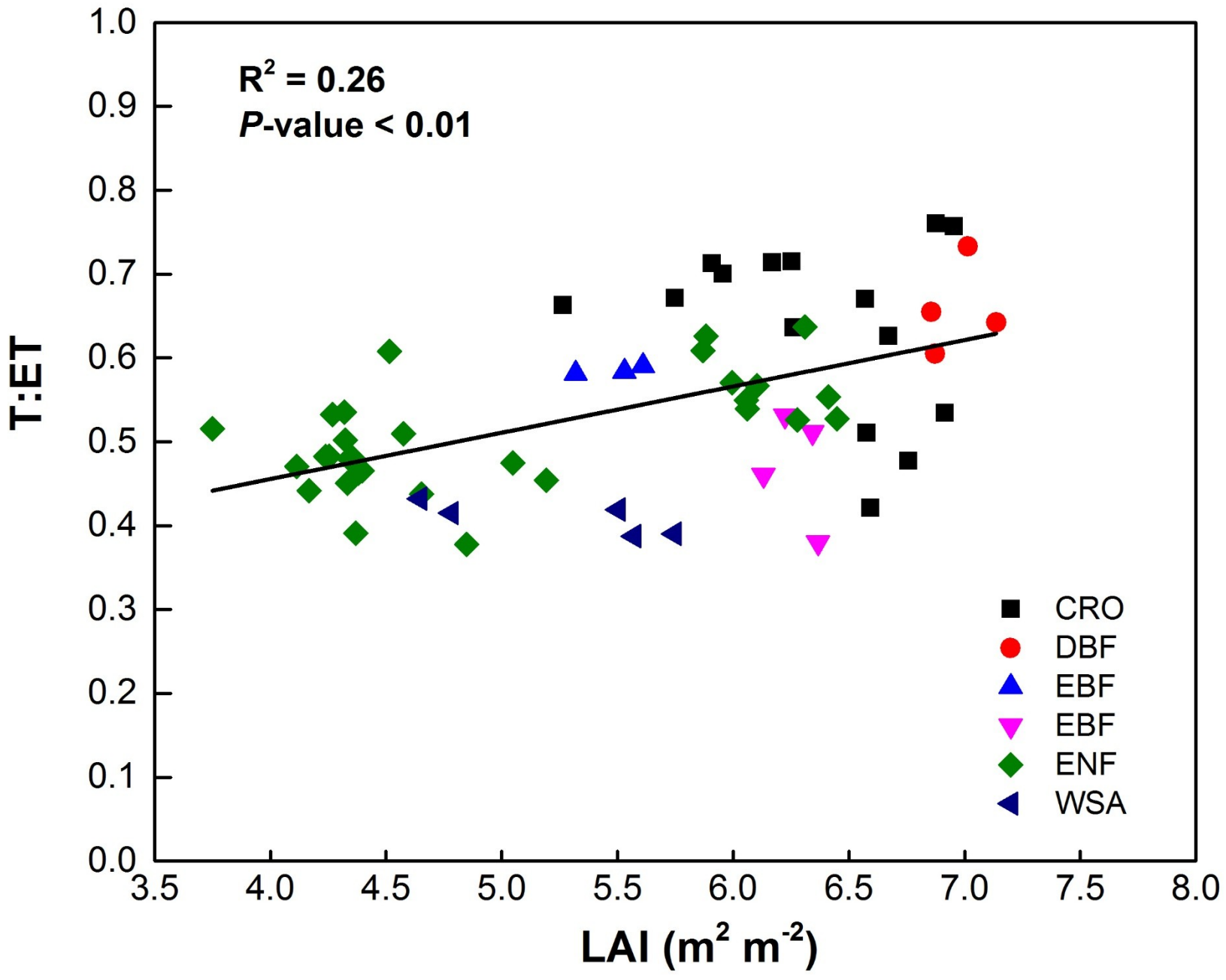

386

387 **Figure 6.** The comparison of *T:ET* estimation among various methods. The rectangle represents the ranges of *T:ET* values and the value

388 corresponding to the horizontal line in the middle represents the average value of *T:ET* reported in the published literature.

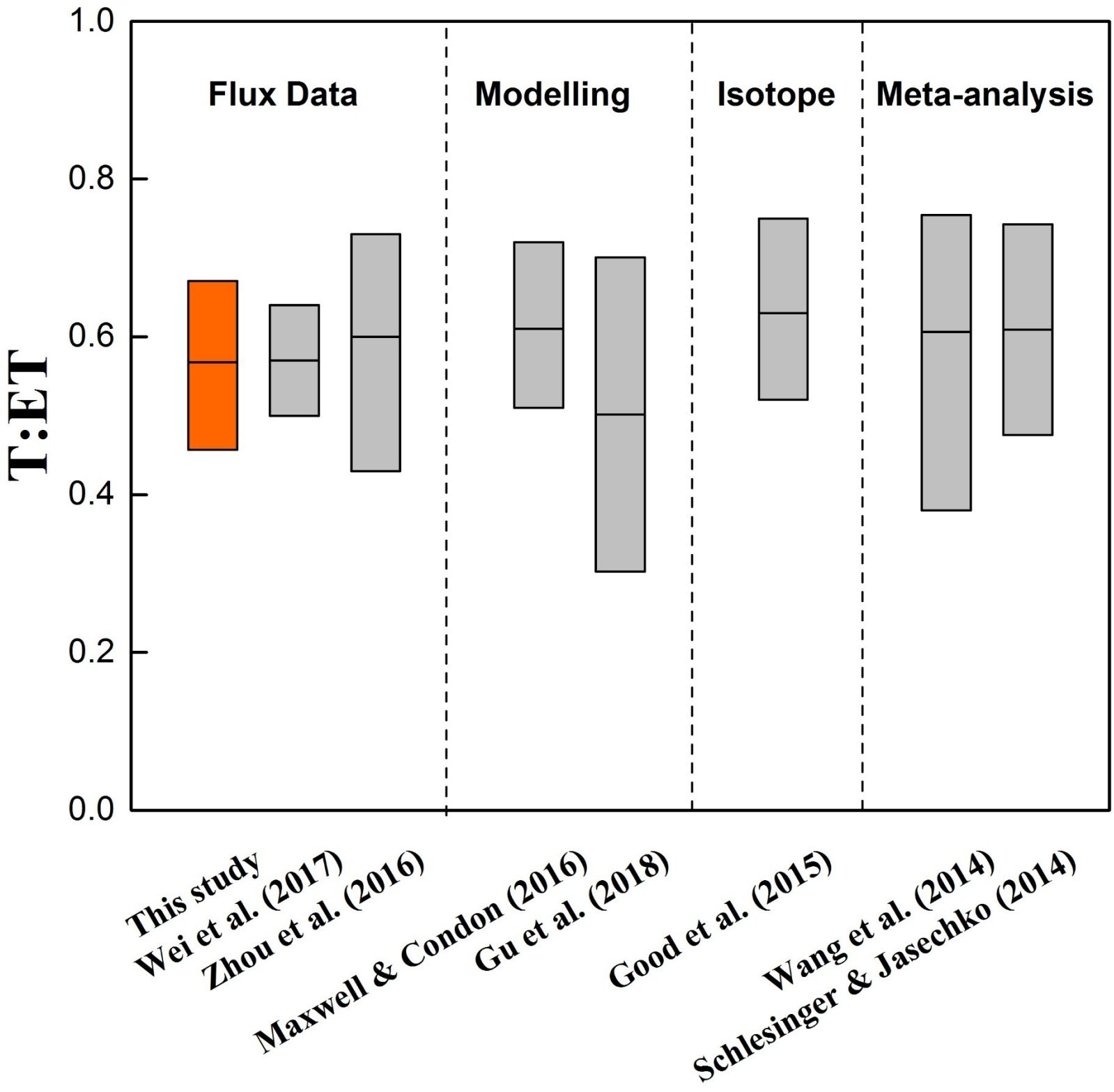

389

390 **Figure 7.** Comparison of *T:ET* estimations on a daily scale between two arid grassland sites in this study (T:ET_Y) and Zhou's method
391 (T:ET_Z). The points located at the (a) US_SRG and (b) US_Wkg sites are 1,987 and 2,591, respectively. The blue dotted line represents
392 the 1:1 trend line. The red line represents the linear equation estimated using orthogonal-least-squares regression.

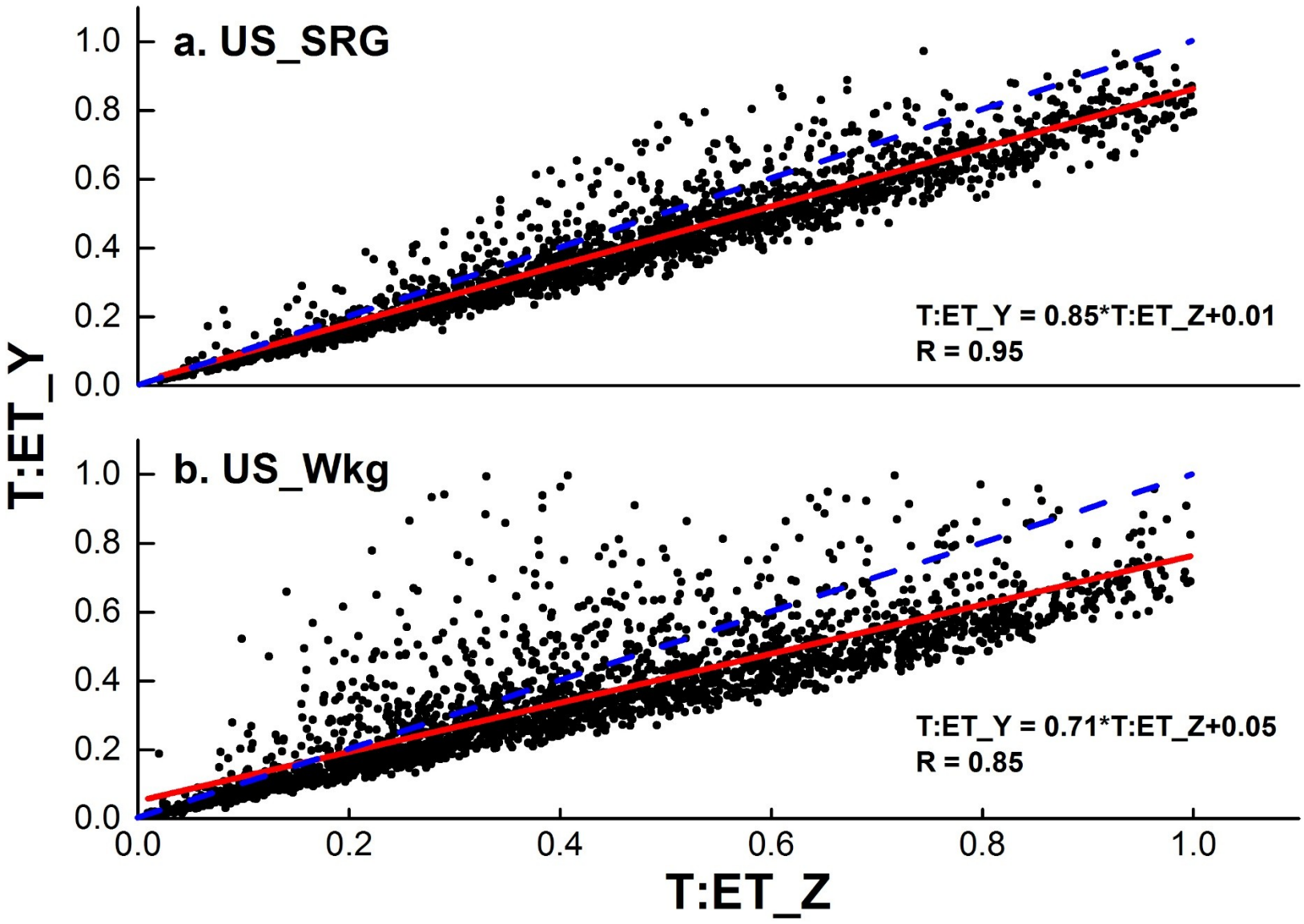

393

394 **Figure 8.** Comparison of daily *T:ET* characteristics in 2010 between two arid grassland sites in this study (T:ET_Y) and Zhou's method

395 (T:ET_Z). The difference is expressed as *T:ET* value estimated by Zhou's method minus *T:ET* value estimated by this method.

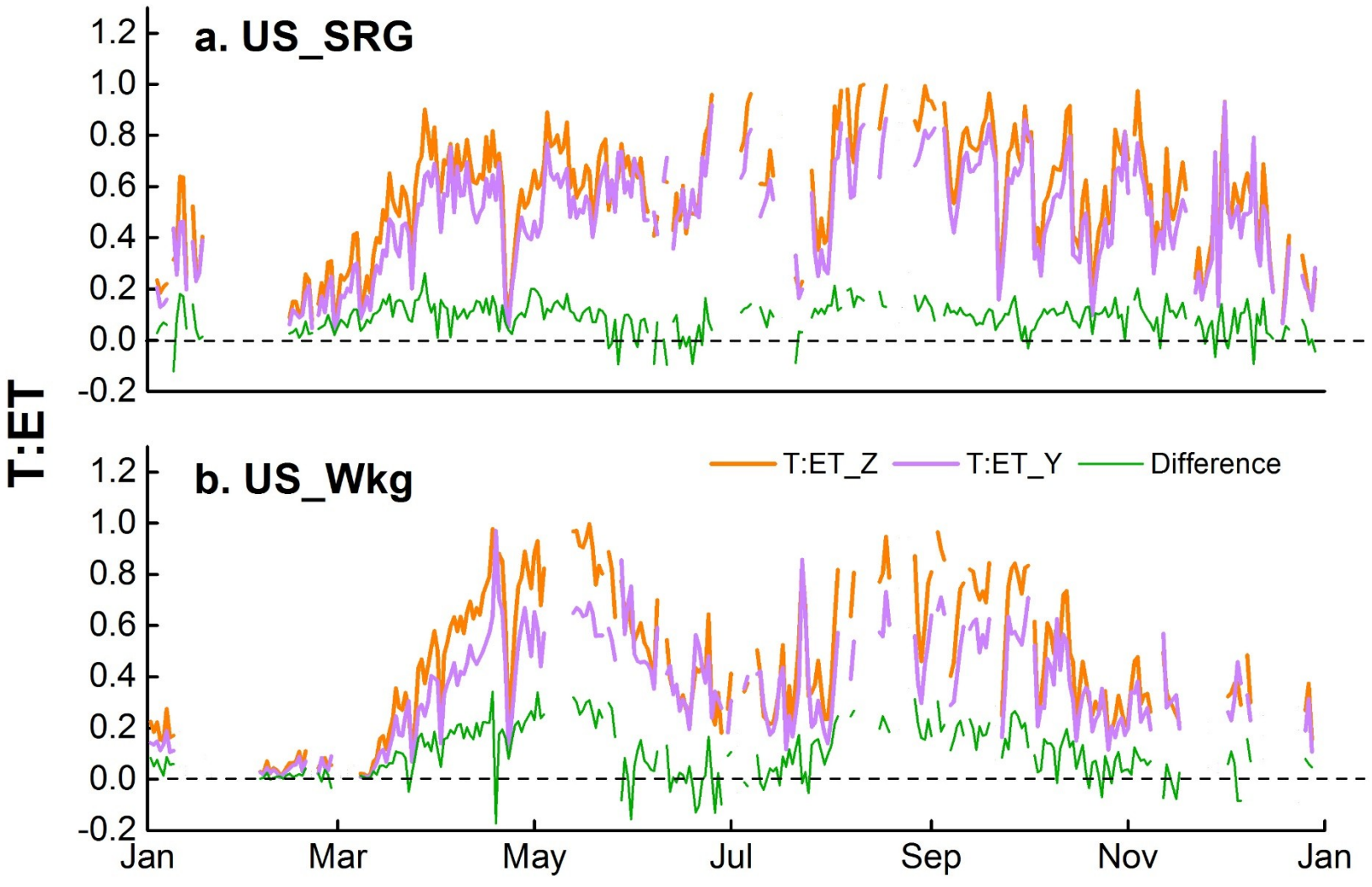

396

397 **Table 1.** Information of the 25 fluxnet sites and parameter g_1 used in the study.

SITE CODE	LAT	LON	Elevation (m)	PFT	MAT (℃)	MAP (mm)	g_1 (KPa$^{0.5}$)	YEARS USED	REFERENCE
CA_NS3	55.91	-98.38	260	ENF	-2.87	502.22	2.9	2001-2006	(Bond-Lamberty et al., 2004)
CA_Oas	53.62	-106.19	530	DBF	0.34	428.53	5.1	1997-2010	(Barr et al., 2004)
DE_Gri	50.95	13.51	385	GRA	7.8	901	4.9	2004-2014	(Prescher *et al.*, 2010)
DE_Hai	51.08	10.45	430	DBF	8.3	720	5.5	2000-2009	(Knohl *et al.*, 2003)
DE_Obe	50.79	13.72	734	ENF	5.5	996	5.1	2008-2014	(Zimmermann *et al.*, 2006)
DE_RuS	50.86	6.45	102	CRO	10	700	5.4	2011-2014	(Mauder et al., 2013)
DE_Seh	50.87	6.45	103	CRO	9.9	693	5.4	2007-2010	(Schmidt et al., 2012)
FR_Fon	48.48	2.78	103	DBF	10.2	720	4.7	2012-2014	(Bazot et al., 2013)
FR_Pue	43.74	3.60	270	EBF	13.5	883	3.8	2001-2014	(Rambal et al., 2004)
IT_Cpz	41.71	12.38	68	EBF	15.6	780	3.9	2000-2007	(Garbulsky et al., 2008)
NL_Loo	52.17	5.74	25	ENF	9.8	786	4.7	1997-2014	(Gioli *et al.*, 2004)
US_ARb	35.55	-98.04	424	GRA	/	/	3.5	2005-2006	(Schmidt et al., 2011)
US_ARc	35.55	-98.04	424	GRA	/	/	3.5	2005	(Schmidt et al., 2011)
US_CRT	41.63	-83.35	180	CRO	10.1	849	5.3	2011-2013	(Chu et al., 2016)
US_Goo	34.25	-89.87	87	GRA	15.89	1425.77	4.2	2002-2006	(Benjamin et al., 2017)
US_Ha1	42.54	-72.17	340	DBF	6.62	1071	4.6	1994-2012	(Barford et al., 2001)
US_Ne1	41.17	-96.48	361	CRO	10.07	790.37	1.6	2002-2010	(Suyker *et al.*, 2004)
US_Ne2	41.16	-96.47	362	CRO	10.08	788.89	4.0(C_3)/1.6(C_4)	2001-2012	(Suyker *et al.*, 2004)
US_Ne3	41.18	-96.44	363	CRO	10.11	783.68	4.0(C_3)/1.6(C_4)	2001-2012	(Suyker *et al.*, 2004)
US_NR1	40.03	-105.55	3050	ENF	1.5	800	2.6	2006-2008	(Arain et al., 2005)
US_SRG	31.79	-110.83	1291	GRA	17	420	3.7	2008-2014	(Biederman *et al.*, 2016)
US_SRM	31.82	-110.87	1120	WSA	17.92	380	3.7	2011-2013	(Scott et al, 2010)
US_Ton	38.43	-120.97	177	WSA	15.8	559	3.3	2003-2005	(Fisher *et al.*, 2007)
US_UMB	45.56	-84.71	234	DBF	5.83	803	4.7	2000-2014	(Curtis et al., 2007)
US_Wkg	31.74	-109.94	1531	GRA	15.64	407	3.9	2004-2012	(Moran *et al.*, 2009)

398

399 Note: Site code, Latitude (LAT, °), longitude (LON, °), elevation (m), plant functional type (PFT), MAP (mean annual precipitation), MAT
400 (mean annual temperature), g_1 (parameter of the Ball stomatal conductance model), years used and corresponding reference are listed. The
401 PFTs include croplands (CRO), deciduous broadleaf forests (DBF), evergreen broadleaf forests (EBF), evergreen needleleaf forests (ENF),
402 grasslands (GRA) and woody savannas (WSA).

403

Table 2. Comparison of monthly and growing season *T:ET* among Scott and Biederman, 2017, Zhou *et al.*, 2015 and this study at the US_SRG (2008-2015) and US_Wkg (2004-2015) sites.

Site	Study	July	August	September	October	Growing Season	Difference (%)
US_SRG	Scott and Biederman, 2017	0.54	0.62	0.54	0.51	0.55	/
	This study	0.55	0.63	0.55	0.52	0.56	+ 1.82
	Zhou et al., 2015	0.64	0.73	0.6	0.6	0.64	+ 14.3
US_Wkg	Scott and Biederman, 2017	0.26	0.58	0.54	0.45	0.46	/
	This study	0.35	0.52	0.48	0.46	0.45	- 0.3
	Zhou et al., 2015	0.48	0.66	0.66	0.69	0.62	+ 37.8

Note: The two grassland sites are in water-limited regions where mean annual precipitation is 420 and 407 mm. The difference (%) is expressed as the percent of the *T:ET* difference values relative to the results of Scott and Biederman (2017).